Materials Today Energy 38 (2023) 101426

Contents lists available at ScienceDirect

Materials Today Energy

journal homepage: www.journals.elsevier.com/materials-today-energy/

On the shoulders of high-throughput computational screening and machine learning: Design and discovery of MOFs for H_2 storage and purification☆

Cigdem Altintas, Seda Keskin☆

Department of Chemical and Biological Engineering, Koc University, Rumelifeneri Yolu, Sariyer, 34450, Istanbul, Turkey

ARTICLE INFO

Article history:
Received 9 August 2023
Received in revised form
11 September 2023
Accepted 20 September 2023
Available online 22 September 2023

Keywords:
Metal organic frameworks
Hydrogen storage
Molecular modeing
Machine learning

ABSTRACT

Hydrogen (H_2) is a promising energy carrier for achieving net zero carbon emissions. Metal organic frameworks (MOFs) and covalent organic frameworks (COFs) have emerged as strong alternatives to traditional porous materials for highly efficient H_2 storage and purification applications. With the very rapid and continuous increase in the number and variety of MOFs and COFs, early studies in this field focused on experimental testing of a few types of randomly selected materials have recently evolved into studies combining computational screening of very large material databases with machine learning (ML). In this review, we highlighted the recent trends in merging molecular modeling and ML in the field of MOFs and COFs for H_2 storage and purification. After reviewing high-throughput computational screening studies aiming to determine the best material candidates for H_2 adsorption and separation, we discussed the recent studies that use ML for extracting hidden structure–performance relations from molecular simulation results to provide new guidelines for the inverse design of novel MOFs. Finally, we addressed the current opportunities and challenges of fusing data science into molecular modeling to speed the development of innovative adsorbent and membrane materials for H_2 storage and separation, respectively.

© 2023 The Author(s). Published by Elsevier Ltd. This is an open access article under the CC BY-NC-ND license (http://creativecommons.org/licenses/by-nc-nd/4.0/).

1. Background

Utilization of hydrogen (H_2) as a clean and effective energy carrier under safe operating conditions is an ambitious goal in the pursuit of transportation with net zero emissions for which extensive research and development efforts are currently underway [1–3]. H_2 has a low volumetric energy density compared to other fuels (8 MJ/L for liquid H_2; 32 MJ/L for gasoline) [4] and a high amount of H_2 has to be stored on-board to attain a driving range competitive to the conventional technologies. The U.S. Department of Energy (DOE) defined gravimetric (kg H_2 per mass of material) and volumetric (kg H_2 per volume of material) H_2 capacity targets for the on-board H_2 storage systems, and both targets should ensure that the on-board H_2 storage setup will be neither too large nor too heavy. The overall system should have a gravimetric H_2 capacity of 6.5 wt% and volumetric capacity of 50 g H_2/L to compete with the conventional technologies while the target for 2025 is set as 5.5 wt% and 40 g H_2/L [5].

Thermodynamic-based (high pressure or cryogenic temperatures) and material-based (sorbents, hydrides, nanostructured materials) approaches offer many possibilities to investigate the most efficient H_2 storage conditions and medium [6]. Among different types of materials, metal organic frameworks (MOFs) have emerged as a strong alternative to traditional porous materials. MOFs are a distinct family of crystalline materials obtained through the coordination of metal nodes with organic linkers and they offer large structural and chemical diversities that can be tuned for a target application [7–10]. Currently, we are aware of almost 120,000 different types of experimentally synthesized MOFs [11–13], while the number of hypothetically designed, computer-generated but not synthesized yet MOFs, even exceeds millions [14–16]. This enormous materials space offers a huge potential for H_2 storage via adsorption [17–20].

The first synthesized proto-type MOF, (isoreticular metal organic framework) IRMOF-1 (also known as MOF-5), was reported to have a high H_2 saturation capacity of 4.7 wt% at 50 bar, 77 K [21]. This early discovery highlighted the importance of the MOF–H_2

☆ Submitted to *Materials Today Energy*.

☆ Corresponding author.
E-mail address: skeskin@ku.edu.tr (S. Keskin).

https://doi.org/10.1016/j.mtener.2023.101426
2468-6069/© 2023 The Author(s). Published by Elsevier Ltd. This is an open access article under the CC BY-NC-ND license (http://creativecommons.org/licenses/by-nc-nd/4.0/).

interactions during adsorption at low pressures and the prominence of available surface area of the MOF which determines the H_2 saturation capacity at high pressures. Further studies showed that depending on the synthesis conditions, even higher gravimetric and volumetric capacities, up to 10 wt% and 66 g/L at 100 bar and 77 K, could be achieved with MOF-5 [22]. Hydrogen Storage Engineering Center of Excellence [23], which was established to focus on engineering challenges related to H_2 storage and provide system modeling tools, has shown that MOF-5 offers a superior performance to reach the DOE targets in various scenarios [24]. A beryllium-based MOF was shown to have an exceptional H_2 storage capacity of 6 wt% at 20 bar, 77 K with a volumetric capacity of ~35 g/L [25]. MOF-177 and IRMOF-20 are among the other promising materials achieving very high gravimetric (7.5 and 6.7 wt%, respectively) and volumetric (32 g/L and 34 g/L, respectively) capacities at ~80 bar, 77 K [26].

Covalent organic frameworks (COFs), which can be considered as the non-metal versions of MOFs, offer better chemical robustness than MOFs because of the presence of covalently linked organic units in their crystalline structures [27,28]. A much smaller number of COFs (~650) [29,30] has been experimentally synthesized than MOFs while the number of hypothetically designed COFs has already reached hundreds of thousands [31–33]. High accessible surface area and extremely low density of COFs have suggested that they can have even superior H_2 storage performances than MOFs [34]. An early experimental work [35] on COF-5 reported a H_2 capacity of 3.5 wt% at 50 bar, 77 K and many other COFs (COF-1, -6, -8, -10) were shown to have H_2 uptakes of <4 wt%, while COF-102 and COF-103 were discovered to have high H_2 saturation capacities near 7 wt% at ~40 bar, 77 K [36]. Several excellent reviews addressed the potential of MOFs and COFs for H_2 storage and highlighted the strategies for improving H_2 storage performance of these materials by structural modifications during or after their synthesis [37–40].

Fig. 1 represents different types of methodologies implemented to study MOFs and COFs for H_2 storage and separation applications in the literature; experiments, computational simulations and very recently, machine learning (ML). Due to the very large material space of synthesized and hypothetical MOFs and COFs, it is not practical to conduct experiments for every single material. Studying H_2 adsorption requires very low temperatures and very high pressures to determine the maximum deliverable capacities of materials and defining the optimal conditions for a high deliverable H_2 capacity requires iterative experiments. The computational methods, specifically molecular simulations that provide a quick and an accurate assessment of H_2 adsorption in porous materials, are highly useful. Since 2012, MOFs have been studied intensively for H_2 storage and half a thousand of distinct articles has been published. Almost 20% of these articles utilized molecular simulations, which also provide molecular level insights into the material–H_2 interactions which are not directly observable at the length and timescale of the experiments. However, the number of materials is increasing too rapidly to perform brute-force molecular simulations in addition to the difficulty of analyzing the very large simulation data to extract useful information. ML algorithms can be very useful when combined with molecular simulations to predict the H_2 adsorption capacity of large number of MOFs in addition to estimate MOFs' performances for H_2 separation from various other gases such as CH_4, H_2S, and CO_2. Therefore, early studies focusing on experimental testing of a few types of randomly selected materials have recently evolved into studies combining computational screening of very large material databases using molecular simulations and ML, which all complement each other to provide a comprehensive chemical insight into the field.

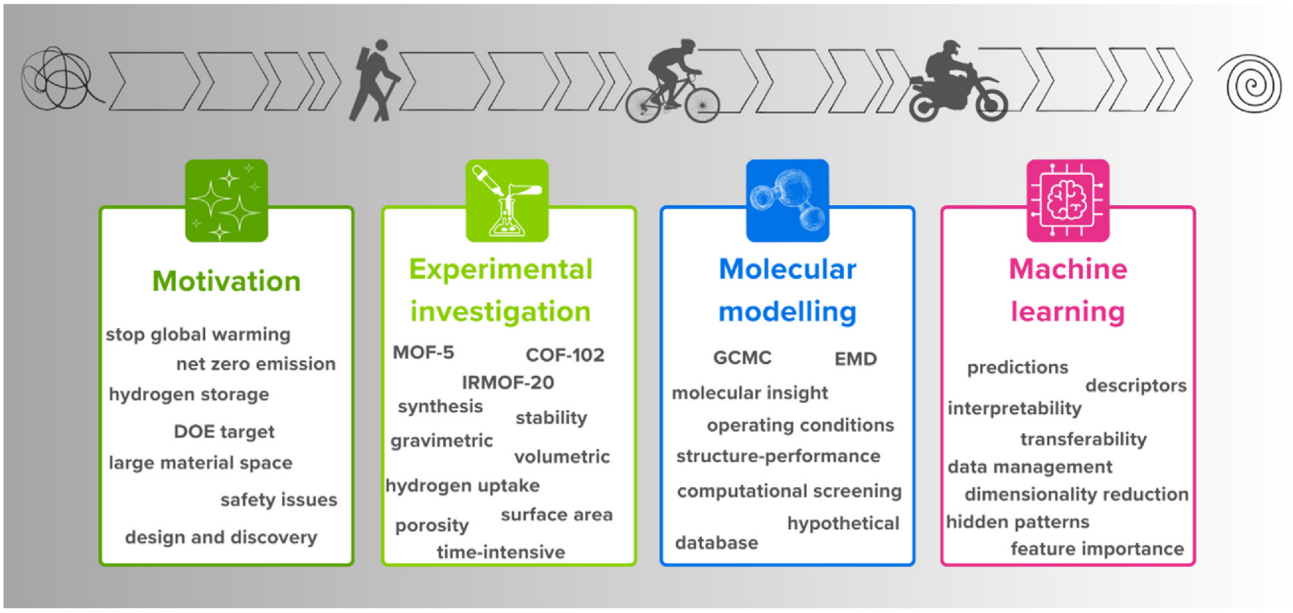
In this review, we aimed to highlight the recent trends of combining molecular modeling and ML in the field of H_2 storage and purification using MOFs and COFs. We first reviewed the high-throughput computational screening (HTCS) studies to identify the best material candidates for H_2 storage and separation. We then addressed the recent studies combining ML with molecular modeling to extract the quantitative structure–performance relations from the molecular simulation results and to provide new guidelines for the inverse design of new materials that can offer high-performance for efficient storage and separation of H_2. We finally addressed the opportunities and challenges of incorporating data science into molecular modeling to accelerate the discovery of novel adsorbent and membrane materials for H_2 storage and separation.

2. HTCS of MOFs and COFs

2.1. H_2 storage

Almost all the computational studies use Grand Canonical Monte Carlo (GCMC) simulation technique to compute H_2 adsorption in MOFs since GCMC has been proven to be useful for accurately computing gas adsorption in porous materials and complementing the experimentally measured gas adsorption isotherms [41,42]. The input of a GCMC simulation are the crystallographic information file (CIF) of the MOF (can be taken from the publication reporting the synthesis of the MOF, or from a computation-ready MOF database such as CoRE-MOF [11,43] which provide the CIFs in a format ready to be used in the molecular simulations, or from Cambridge Structural Database [44] which reports the CIFs of MOFs deposited into the datacenter), potentials for the H_2 molecule (such as Buch's [45], Darkrim and Levesque's [46] potential) and MOFs (such as Universal Force Field [47] and Dreiding [48]) in addition to the temperature and pressure of the adsorption process. To determine the set of input parameters to be used in a GCMC simulation, it is a generally adopted approach to compare and validate the gas uptakes obtained from the GCMC simulation with the gas uptakes measured by experimental methods at the same temperature and pressure [49,50]. GCMC simulations output adsorbed H_2 amount in a MOF at a given condition in addition to the heat of adsorption, an indicator of adsorbent–gas interactions at low loadings. The adsorbed H_2 amount can be further used to calculate the deliverable H_2 capacity of a material, which is the amount of H_2 released between adsorption and desorption pressures.

In the early computational studies, GCMC simulations were performed to evaluate the H_2 storage performances of only a handful of MOFs and COFs [51–55]. These studies also provided molecular-level insights into the most important structural features of materials that determine their H_2 storage capacities. By GCMC simulations, Frost and Snurr [51] computed gravimetric and volumetric H_2 capacities of 10 different IRMOFs and showed that heat of adsorption, surface area, and pore volume play a significant role on H_2 adsorption at low (~0.1 bar), intermediate (~30 bar), and high (~120 bar) pressure, respectively. H_2 adsorption in MOFs and COFs generally occur thorough physical adsorption, also known as physisorption. Three different mechanisms, monolayer formation in micropores (<20 Å), pore filling, and capillary condensation in mesopores, can define the H_2 storage capacity of a porous adsorbent depending on the adsorbent–H_2 interactions [56]. Adsorption mechanism of H_2 in three MOFs, NU-1101, NU-1102, NU-1103, was investigated using GCMC simulations, and it was shown that volumetric surface area and pore volume of MOFs should be maximized together to achieve both high gravimetric and volumetric deliverable capacities [19]. An early computational work on



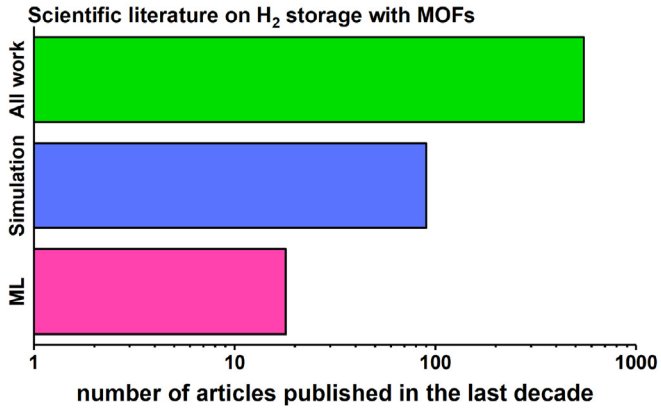


Fig. 1. The research track on the investigation of MOFs and COFs for H_2 storage and purification applications in the last decade. The number of articles published between 2012 and 2022 was retrieved using the combination of the search terms 'metal organic framework' and 'hydrogen storage' or 'H_2 storage' as represented in green bar, 'metal organic framework' and 'hydrogen storage' or 'H_2 storage' and 'simulation' as represented in blue bar, 'metal organic framework' and 'hydrogen storage' or 'H_2 storage' and 'machine learning' as represented in magenta bar. Search results were limited to articles (Scopus, accessed on June 29th, 2023). COF, covalent organic framework; MOF, metal organic framework.

COF adsorbents for H_2 storage has shown that the chemical features of the materials, such as the type of the organic linkers, is important and benzene rings on organic linkers provide favorable adsorption sites for H_2 molecules at low pressure [35].

Rapidly and unpredictably increasing number of experimentally synthesized and hypothetically designed MOFs in addition to the developments in the computational tools and advancement in computational power accelerated the efforts toward the HTCS of materials for H_2 storage [57,58]. HTCS is an approach where performances of thousands of materials can be quickly obtained and the most promising material candidates for a specific application can be identified based on the predefined performance metrics. H_2 adsorption is widely investigated at cryogenic temperatures since H_2 has a more tendency to adsorb at 77 K than at room temperature, which can ultimately result in higher H_2 capacities at lower pressures. In the first example of HTCS of MOFs for H_2 storage, Goldsmith et al. [59] computed the surface area of 22,700 MOFs compiled from the CSD (Cambridge Structural Database) and then estimated both gravimetric and volumetric H_2 uptake of MOFs at 35 bar, 77 K using the Chahine rule, which defines a linear relationship between accessible surface area and H_2 capacity of materials at cryogenic temperatures [60,61]. 78 MOFs exceeded the DOE target with gravimetric uptakes between 5.5 wt% and 16 wt% and volumetric uptakes between 40 g/L up to ~70 g/L at 77 K and 35 bar. These values represented the total H_2 uptakes at the adsorption pressure but assessing the deliverable capacities is also important to define the exact amount of H_2 that will be useable on-board.

To focus on this point, Bobbitt et al. [62] performed GCMC simulations at 2 bar and 100 bar, at 77 K to screen 137,953 different types of hypothetical MOFs and identified 49 MOFs with a deliverable volumetric capacity above 48 g/L, which is higher than the DOE target for 2025. As shown in Figs. 2(a–b), the range of optimal structural properties of MOFs that lead to a deliverable H_2 capacity higher than the DOE target was identified as void fraction of ~0.9, surface area of ~2000 m^2/cm^3, and heat of adsorption values for H_2 were computed to vary between 2 and 4 kJ/mol in these MOFs. These results highlighted that MOFs with high void fractions can be especially useful for cryogenic temperatures since they provide a low heat of adsorption at desorption conditions, indicating a weak

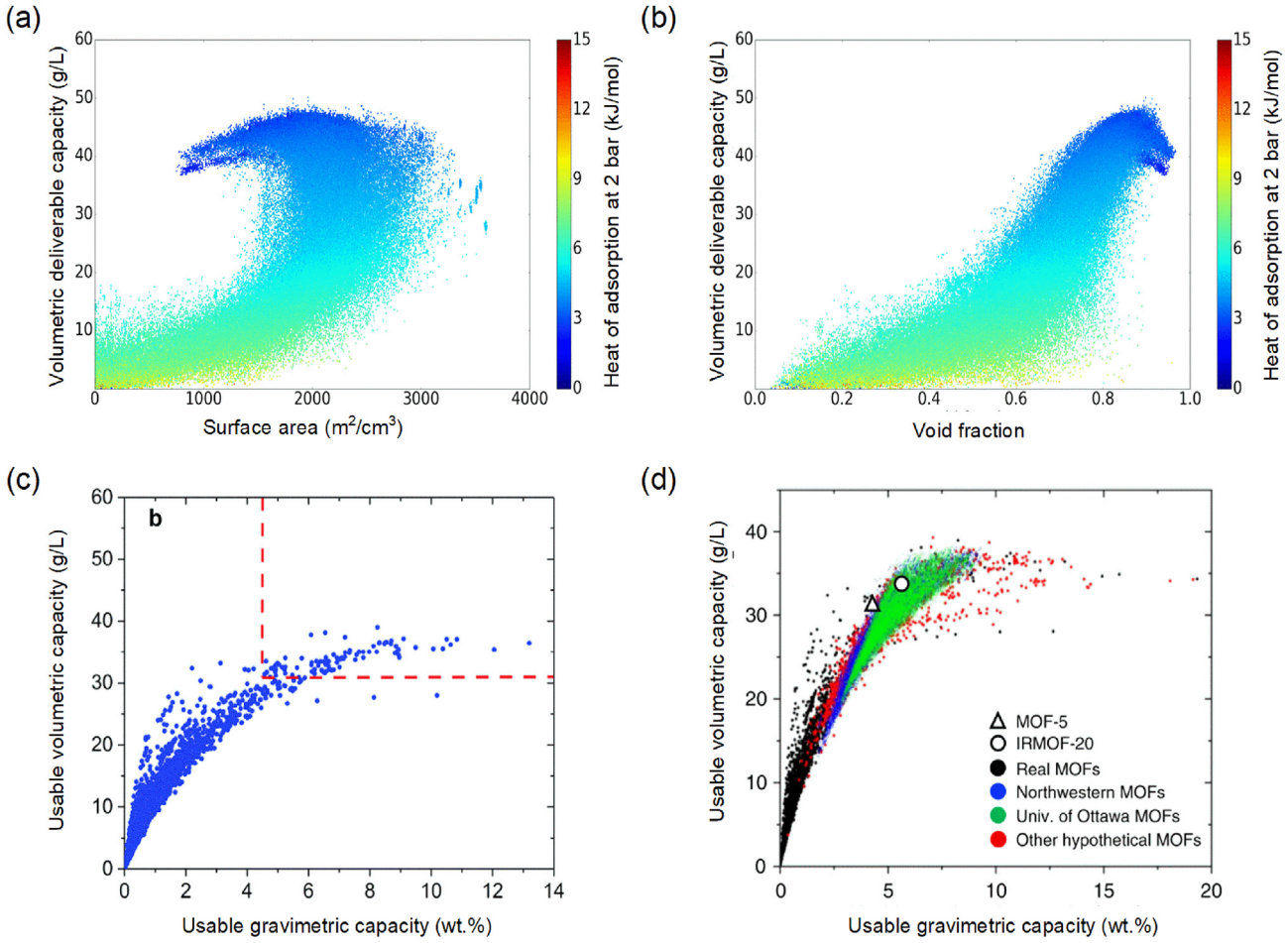


Fig. 2. Impact of (a) surface area and (b) void fraction on volumetric deliverable capacity of 137,953 hypothetical MOFs. Color scale represents the range for heat of adsorption at desorption condition. Figures reprinted with permission from reference. [62] Copyright 2016 American Chemical Society. Further permissions related to the material excerpted should be directed to the American Chemical Society. (c) Relation between gravimetric and volumetric deliverable capacity of 5309 experimentally synthesized MOFs between 100 and 5 bar, at 77 K. Red dashed lines represent the performance of MOF-5. Figure reproduced from Ref. [63] with permission from the Royal Society of Chemistry. (d) Relation between gravimetric and volumetric deliverable capacity of 43,777 experimentally synthesized and hypothetical MOFs between 100 and 5 bar, at 77 K. Figure reprinted with permission from reference. [64] (licensed under CC BY 4.0). MOF, metal organic framework.

MOF–H_2 interaction, leading to a low H_2 uptake at desorption and high volumetric deliverable capacity.

In addition to the structural features, chemical composition such as metal type, linker type, functional groups, and topology collaboratively define the H_2 storage capacities of materials. The diversity of metal types in hypothetical MOF databases was shown to be low and a new hypothetical MOF database composed of ~20,000 structures was generated using 42 different topologies and 14 different nodes with paying particular attention on including the metal types that were not typically found in previous MOF databases [65]. The new database was screened for H_2 storage using GCMC simulations and 50 materials in *tfz-d* topology with eight-coordinated cobalt-based and cadmium-based metal nodes exhibited a favorable balance between gravimetric and volumetric H_2 uptakes (higher than 9 wt% and 52 g/L).

One important factor that defines the deliverable H_2 capacity is MOF–H_2 interaction since it determines the saturation capacity of the material at adsorption pressure and the amount of gas released at desorption pressure. To attain high deliverable H_2 capacities, this interaction should be arranged so that it is neither too strong nor too weak. For improving the adsorbent–H_2 interactions at room temperature, MOFs and porous aromatic frameworks were functionalized by magnesium alkoxide to generate 18,383 hypothetical materials and then examined using GCMC simulations [66]. MOFs with high gravimetric deliverable capacities were found to suffer from volumetric deliverable capacities because materials having porosities close to 0.75 and magnesium densities close to 2.5 mmol/cm^3 offer high volumetric capacities whereas MOFs with high porosities (>0.9) and magnesium densities closer to 0.5 mmol/cm^3 offer high gravimetric capacities.

These HTCS studies showed that structural, geometrical, and chemical properties are critical for the identification of the best materials for H_2 storage. Motivated from this, Gomez et al. targeted to compare the set of promising MOF candidates for H_2 storage identified with different approaches. First, a set of thresholds for MOF density, metal atom density, gravimetric uptake obtained from GCMC simulations was used to narrow down hypothetical MOFs from 137,953 to 152 candidates. The best 10 MOFs with gravimetric H_2 uptake >5.5 wt% at pressures lower than 50 atm were then identified by GCMC simulations between 1 and 100 atm at 77 K [67]. A second set consisting of 8 top materials was obtained as a result of independent screening steps considering only 1411 paddlewheel structures with open metal sites. Two discrete sets of top candidates were then compared and none of the structures identified with the second approach was found with the first approach, highlighting that distinct screening criteria utilized in

HTCS studies will identify a different region of the promising MOF space.

The ultimate motivation of HTCS studies is to direct the experimental efforts, time, and resources to the best material candidates. One good example of combining molecular simulations with experiments is the discovery of *she*-MOF-1 [68]. 13,512 hypothetical MOFs in diverse topologies were generated and screened by GCMC simulations for H_2 storage. The deliverable volumetric H_2 capacity of *she*-MOF-1 was shown to be promising, 50.3 g/L, among 100 bar, 77 K, and 5 bar, 160 K. Synthesizability and stability of *she*-MOF-1 were then studied and a deliverable volumetric capacity of 43.4 g/L was measured, consistent with the simulations.

In a similar manner, Ahmed et al. [63] examined the deliverable gravimetric and volumetric H_2 capacity of 5309 MOFs using the results of GCMC simulations and identified 90 MOFs with deliverable H_2 capacities higher than that of MOF-5 (4.5 wt% and 31 g/L between 5 and 100 bar at 77 K) as shown in Fig. 2(c). IRMOF-20 was one of these materials and its stability and high deliverable volumetric (gravimetric) H_2 capacity of 51 g/L (9.1 wt %) among 100 bar, 77 K, and 5 bar, 160 K was then experimentally validated. The same group later screened half a million of synthesized and hypothetical MOFs retrieved from various databases using HTCS and then experimentally validated the deliverable H_2 capacities of the most promising MOF candidates [64]. Gravimetric and volumetric H_2 uptakes of 493,458 MOFs were computed using the Chahine rule and 43,777 MOFs offering superior capacity compared to MOF-5 were selected. GCMC simulations on these materials showed that SNU-70, UMCM-9, and PCN-610/NU-100 have deliverable capacities exceeding those of the record-holder MOFs, MOF-5 (4.5 wt% and 31.1 g/L) and IRMOF-20 (5.7 wt% and 33.4 g/L) as shown in Fig. 2(d). Further experimental studies demonstrated that these MOFs offer a good balance between gravimetric and volumetric capacities. These works clearly highlight the great benefit of first-computation approach to narrow down the huge number of materials for directing the very valuable experimental efforts to a handful of promising candidates and the importance of collaborations between experimentalists and theoreticians.

2.2. H_2 separation

Many of the current HTCS studies focused on the H_2 storage performances of MOFs. However, H_2 is not pure under real conditions and exist with other gas molecules [69–73]. Therefore, purification of H_2 from methane (CH_4), carbon dioxide (CO_2), and nitrogen (N_2) is very critical. Thanks to the large variety of pore sizes, shapes, and functionalities of MOFs, they also hold great promise for adsorption-based and membrane-based separation of H_2 from other gases. To assess adsorption-based H_2 separation performances of MOFs, gas uptakes obtained from GCMC simulations are used to compute the adsorbent selectivities. However, H_2 is generally weakly adsorbed in MOFs compared to CH_4, N_2, and CO_2, and therefore, most of the MOF adsorbents are not H_2-selective in the adsorption. Our group studied 4350 MOFs [13] by computing their adsorbent performance evaluation metrics such as adsorption selectivity, working capacity, adsorbent performance score, percent regenerability, and sorbent selection parameter based on the results of GCMC simulations for adsorption-based separation of H_2 from CH_4 [70]. The correlation between the selectivity and structural properties of MOFs was used to derive a simple mathematical model that can quickly predict the selectivity of MOF adsorbents based on easily computable properties such as the largest cavity diameter and porosity of MOFs and the difference of isosteric heats of adsorption of two gas species adsorbed in MOFs.

Highly selective adsorbent candidates for the separation of an equimolar mixture of H_2 and CO_2 were investigated by performing GCMC simulations on 1092 hypothetical MOFs having open copper sites [49]. MOFs offering high H_2 uptakes were shown to have pore sizes in the range of 10–15 Å since large pores provide more space for the filling of H_2 molecules whereas MOFs having high CO_2/H_2 selectivities generally have pore limiting diameters between 7 and 11 Å, porosity of ~0.8, and surface area between 3500 and 4600 m^2/g. Breakthrough curves are useful to identify the dynamic separation performances of MOFs during adsorption. For the separation of CO_2/H_2 mixture, breakthrough curves were obtained in the same work by simulating a fixed bed column packed with the most promising MOF candidates. Results showed that H_2 can be obtained with high purity in the outlet when the inlet concentration of CO_2 is low since H_2 does not adsorb strongly in the column and leaves earlier than CO_2.

Hydrogen isotope separation is essential since deuterium (D_2) is required for nuclear-fusion based energy; however, separating D_2 from H_2 is a difficult operation due to the identical nature of these two molecules. 929 MOFs with open copper sites were investigated for adsorption-based D_2/H_2 separation at 1 bar, 40 K [74]. MOF adsorbents were found to be D_2 selective with selectivities between 2 and 70 while several MOFs overcome the selectivity of the benchmark MOF, MIL-53-Al (having D_2/H_2 selectivity of ~14 at 0.01 bar, 40 K) [74]. Anion pillared MOF database [75] consisting of 936 MOFs was also investigated for equimolar D_2/H_2 mixture separation [76]. A top candidate MOF, SIFSIX-18-Cd, which was computationally identified to have a D_2/H_2 selectivity of 12 at 1 bar, 40 K, was finally experimentally synthesized and proposed as a promising adsorbent for D_2/H_2 separation with its proven structural stability and hydrophobic character.

To assess membrane-based H_2 separation performances of MOFs, molecular diffusivities of gases through the pores need to be calculated. Equilibrium molecular dynamics (EMD) simulations are generally performed to calculate the diffusion coefficients of gases where the adsorbed gas loadings calculated by the GCMC simulations are used as the input. The results of GCMC and EMD simulations are combined to compute the permeabilities of gases through the MOF membranes. H_2 is generally the highly permeating component thanks to its high diffusivity; therefore, a significant portion of MOF membranes are found to be H_2-selective. The first work that combines GCMC and EMD simulations to study H_2/CH_4 separation performances of 4240 MOF membranes showed that adsorption strongly favors CH_4 over H_2 while diffusion generally favors H_2 over CH_4 at infinite dilution condition. As a result, most of the MOF membranes were found to be CH_4 selective while a significant number of membranes (~1500) were found to be H_2 selective as depicted in Fig. 3 (a). MOFs with pore sizes between 3.8 and 6 Å, porosity between 0.5 and 0.75, and surface area below 1000 m^2/g offered high H_2 permeabilities (>10^4 Barrer) and high H_2/CH_4 selectivities (>10), overcoming the performance limit of polymeric membranes as shown in Fig. 3 (b) [69].

Several works investigated both the adsorbent-based and membrane-based separation performances of MOFs. 11,129 hypothetical MOFs which contain multivariate linkers and up to three types of different functional groups (-F, $-NH_2$, $-OCH_3$) were computationally screened for the separation of equimolar CH_4/H_2 and N_2/H_2 mixtures combining GCMC and EMD simulations [77]. Results showed that both adsorbents and membranes selectively separate CH_4 from H_2. Top performing MOF candidates identified for N_2/H_2 separation in the same work provided selectivities up to 12 for adsorption-based separation. Similar efforts for studying synthesized COFs as adsorbents and membranes showed that COF adsorbents offer a lower CH_4/H_2 selectivity, up to 102 at 1 bar, 298 K as shown in Fig. 3(c), compared to MOF adsorbents (CH_4/H_2

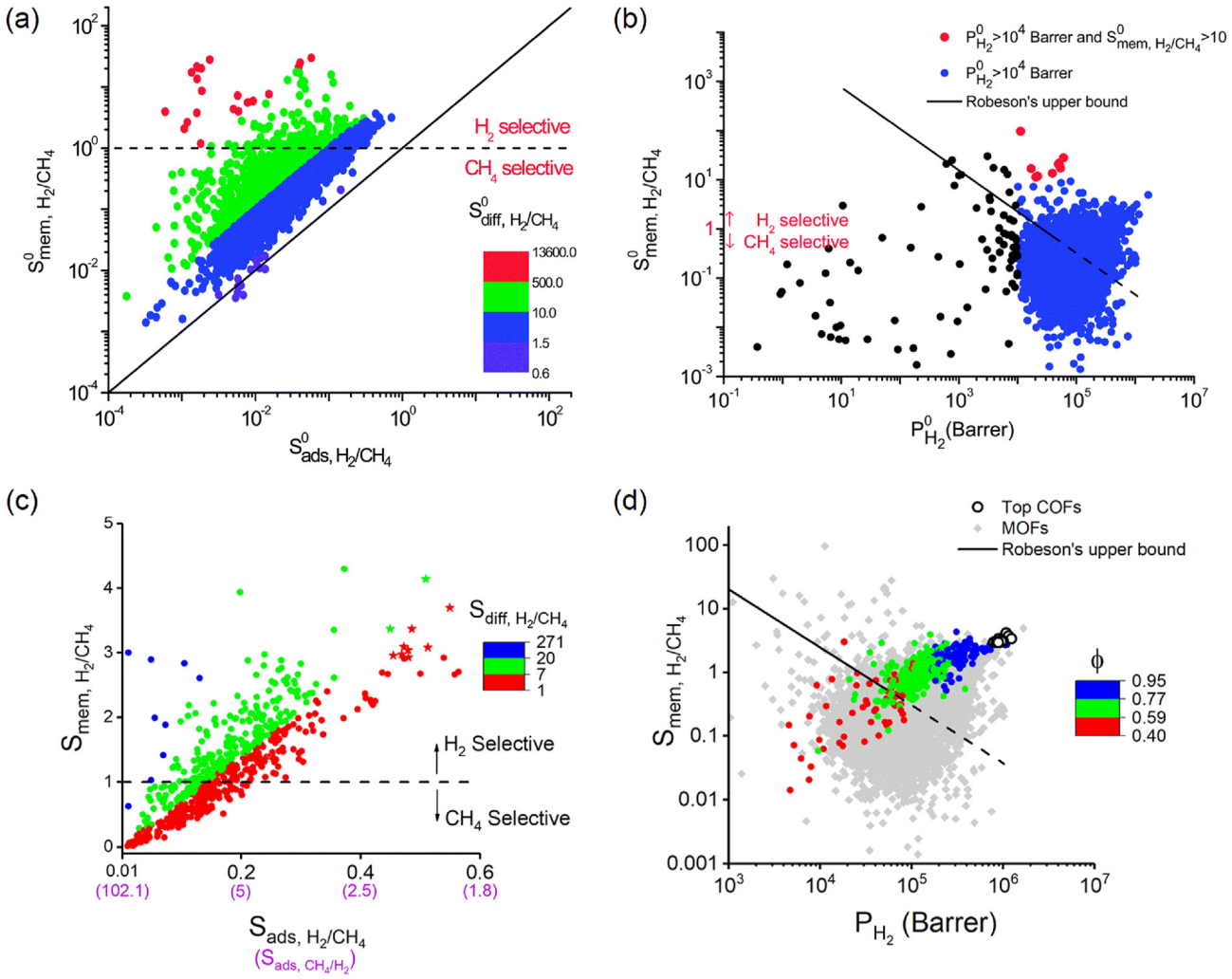


Fig. 3. (a) Relation between adsorption and membrane selectivities of MOFs. Color scale represents the range of diffusion selectivities of MOFs for H_2/CH_4 separation. Figure reproduced from the study by Altintas et al. [69] with permission from the Royal Society of Chemistry. (b) H_2 permeabilities and H_2/CH_4 selectivities of MOF membranes. Figure reproduced from the study by Altintas et al. [69] with permission from the Royal Society of Chemistry. (c) Adsorption and membrane-based separation performances of COFs for selective separation of H2 from CH4 at 1 bar, 298 K. Color scale represents diffusion selectivity of COFs. Figure reprinted with permission from the study by Altundal et al. [78] (licensed under CC BY-NC-ND 4.0) (d) H_2 permeabilities and H_2/CH_4 selectivities of COF membranes at 1 bar, 298 K. Data points were colored according to the porosity. Hollow symbols represent the top COF membranes while gray data points represent the H_2/CH_4 separation performances of MOF membranes computed at infinite dilution condition. Figure reprinted with permission from the study by Altundal et al. [78] (licensed under CC BY-NC-ND 4.0) Solid black lines in (b–d) represent the performance limit of polymer membranes (Robeson's upper bound) for H_2/CH_4 separation. COF, covalent organic framework; MOF, metal organic framework.

selectivity up to ~10,000 at 1 bar, 298 K) whereas COF membranes overcome the performances of high-performing MOF membranes with their H_2/CH_4 selectivities up to ~4 accompanied with H_2 permeabilities up to 1.2×10^6 Barrer for the separation of an equimolar H_2/CH_4 mixture as shown in Fig. 3(d) [78].

For adsorption-based and membrane-based H_2/CO_2 mixture separation, 3857 MOFs retrieved from CSD non-disordered MOF database were examined using GCMC and EMD simulations [71]. One important outcome of this work was that all MOF adsorbents were found to be CO_2 selective (CO_2/H_2 selectivities up to 8.5×10^4 at 1 bar), while in membrane-based gas separation, H_2-selective MOF membranes with high H_2 permeabilities (up to 10^6 Barrer) and H_2/CO_2 selectivities up to 6 exist. Results showed that adsorbent candidates for the selective CO_2 separation from H_2 had narrow pores (<7.5 Å) while a substantial number of MOFs with large pores (>15 Å) and high porosities can overcome the performances of polymers as H_2-selective membranes. In a follow-up work [79], the updated CSD MOF database consisting of 10,221 MOFs was studied and a significant portion of new materials were shown to act as CO_2-selective adsorbents and H_2-selective membranes, indicating the importance of using the latest material databases. COFs were also investigated for the purification of H_2 from CO_2. 288 COF adsorbents were investigated under five different operating conditions for the purification of H_2 from CO_2 [80]. COFs provided membrane selectivities up to ~5 for selective separation of H_2 from CO_2 which was similar to that of MOFs and superior to zeolite membranes. COFs were also found to offer superior H_2 permeabilities, up to 1.5×10^6 Barrer, compared to those of polymeric membranes.

A large set of MOF membranes (3,765) was investigated for H_2/N_2 separation at 298 K at infinite dilution conditions, where H_2 and N_2 are considered to interact only with the framework [72]. The top 20 MOF membranes which exceed the permeability–selectivity trade-off of polymeric membranes were further investigated for binary H_2/N_2 and quaternary $H_2/N_2/CO_2/CO$ mixture separations. Top MOF membranes were used as fillers in various polymers and

these mixed matrix membranes (MMMs) were computed to have double H_2 permeability compared to pure polymers.

GCMC and EMD simulations were combined to evaluate the performances of COF membranes for six different gas separations including the separation of helium (He), N_2, and CH_4 from H_2 [81]. COF membranes showed selectivities up to 3.5, 6.3, and 15.7 for He/H_2, H_2/N_2, and H_2/CH_4 separations, respectively. A set of experimentally synthesized and hypothetical COFs were studied as fillers in 25 different polymers and many COF/polymer MMMs and hypothetical COF/polymer MMMs were shown to overcome the permeability–selectivity trade-off of polymeric membranes with He/H_2, H_2/CH_4, H_2/N_2, and selectivities up to 4.4, 325, and 960, respectively. Using MOFs and COFs as dual fillers in MMMs were also examined for H_2/N_2, H_2/CH_4, and H_2/CO_2 separations and results showed that many MOF/COF/polymer MMMs can overcome the permeability–selectivity trade-off of polymer membranes when dual fillers are used instead of only COF filler [82].

All these studies used EMD simulations to compute the transport coefficients of gas molecules in a MOF or COF membrane. Non-equilibrium molecular dynamics (NEMD) simulations mimic an experimental membrane system by considering the mass transfer resistances through pore openings and make more realistic predictions for the membrane performances of materials. However, NEMD is not applied to a large set of MOFs due to the significant computational time requirement for describing non-equilibrium behavior in large and complex systems. Single-component and binary mixture H_2 and CH_4 permeabilities obtained from NEMD simulations were shown to be in a perfect agreement with the experimental measurements whereas GCMC and EMD approach generally overestimated the permeabilities [83]. For instance, MOF-5 membrane was identified as almost non-selective (H_2/CH_4 selectivity of ~1) based on GCMC and EMD results, but NEMD simulations indicated that it would perform as a H_2 selective membrane with H_2/CH_4 selectivity of ~2, which was consistent with the experimental observations.

3. ML modeling of MOFs and COFs

3.1. H_2 storage

As discussed so far, an enormous amount of data on H_2 adsorption, gravimetric and volumetric H_2 deliverable capacity, H_2 permeability, and H_2 selectivity of MOFs and COFs have been generated. Without the use of data-driven modeling, extracting hidden structure–performance relationships from this large data space is not possible. Thus, integration of data science approaches such as ML to molecular simulations of MOFs and COFs has recently started [84–87]. ML is running 'digital experiments' that use algorithms to correlate materials' features with target properties such as their H_2 storage capacities. The four main components of ML-assisted inquiry are database, descriptors, target property, and algorithm. Computation-ready MOF databases, consisting of synthesized or hypothetical MOFs [11,14,43,68,88], have been utilized in ML studies. As the materials' descriptors, geometrical (such as pore volume, surface area, pore size, density), chemical (such as linker and metal type, metal atom density, metal to non-metal ratio), energy-based (such as MOF-H_2 adsorption energy or energy parameter for van der Waals interactions), and topology-based properties have been used. Almost all ML studies investigating H_2 storage first performed HTCS to compute adsorbed H_2 amount in MOFs and then used simulation results as the target data to train ML models. Various algorithms such as linear regression, ridge regression, k-nearest neighbors, gradient boosting, random forests, extremely randomized trees, support vector machines, genetic algorithm, and neural networks have been used to determine H_2 storage properties of MOFs.

Initial ML-integrated HTCS of MOFs for H_2 storage applications focused on easily computed structural characteristics like surface area and porosity. In the first ML study of H_2 adsorption in MOFs [89], a stepwise GCMC-ML procedure was followed as shown in Fig. 4(a) to identify the characteristics that play a key role on the H_2 working capacities of 850,000 materials in nanoporous materials genome consisting of hypothetical and synthesized MOFs, COFs, porous polymer networks, and zeolites. An initial set of 1000 materials were selected among zeolites and their computed density, porosity, surface area, and pore size were used as the structural descriptors. These structural descriptors were combined with gas uptakes obtained from GCMC simulations to train a neural network model which predicts volumetric working capacities of materials, which were then used to estimate the net deliverable energy, the difference of energy obtained from H_2 and energy required to pre-cool and pressurize it. The dataset of gas uptakes obtained from

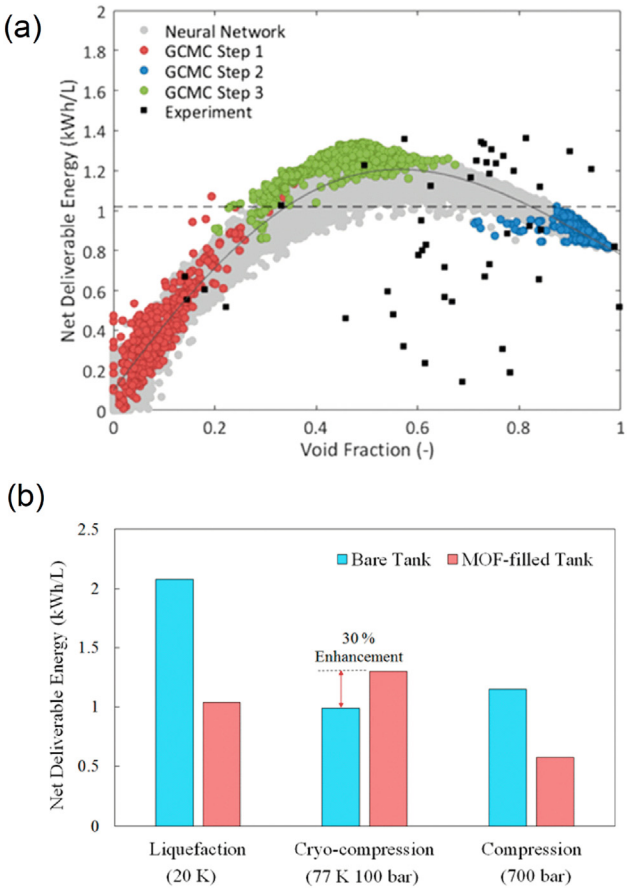


Fig. 4. (a) Net deliverable energy (difference of energy obtained from H_2 and energy required to pre-cool and pressurize it) of ~850,000 materials in Nanoporous Materials Genome with respect to their void fractions. Red, green, and blue data points represent the materials selected in the first, second, and third stage for GCMC simulations, respectively. Gray data points represent model predictions and black squares represent experimental data from the literature including for the MOFs, MOF-210[90], NOTT-400 [91], PCN-68 [92], and ZIF-8 [93]. Figure reprinted with permission from the study by Thornton et al. [89] Copyright 2017 American Chemical Society. Further permissions related to the material excerpted should be directed to the American Chemical Society. (b) Comparison of net deliverable energies for liquefaction, cryo-compression, and compression with and without MOF (hypothetical MOF 5059389) filling. Figure reprinted with permission from the study by Thornton et al. [89] Copyright 2017 American Chemical Society. Further permissions related to the material excerpted should be directed to the American Chemical Society. GCMC, Grand Canonical Monte Carlo; MOF, metal organic framework.

GCMC simulations for an initial set of 1000 zeolites (red data points) was used to obtain model suggestions. A new set of 1000 materials possessing the structural properties that would lead to high deliverable energies were selected and this procedure continued until the model could not predict a material with a higher deliverable energy than the maximum reached. The materials having working capacities up to 40 g H_2/L between 100 and 1 bar at 77 K offered a net deliverable energy up to 1.3 kW h/L, higher than the value proposed by the compression of H_2 in an empty tank at 700 bar, 1.2 kW h/L.

As shown in Fig. 4(b), the material with the highest working capacity of 40 g/L (hypothetical MOF 5059389) provided a 30% gain from the net deliverable energy when it was used for cryogenic compression. MOF-210, NOTT-400, (porous coordination network) PCN-68, and (zeolitic imidazolate framework) ZIF-8 were among the other MOFs identified as the most promising candidates. ML models showed that MOFs with a void fraction of ~0.5, pore size of 10 Å, volumetric surface area of 3000 cm^2/m^3, and gravimetric surface area of 5000 m^2/g are promising. This result highlights the importance of getting a structure−performance map that cannot be directly obtained from the results of pure GCMC simulations without the ML model.

The reliability of ML models significantly depends on the choice and the quality of descriptors used; therefore, accurate reflection of the structural complexity of MOFs using novel descriptors is highly important. Crystal graph convolutional neural networks (CGCNN), which does not require the selection of descriptors and depends only on the structure file (CIF), was implemented besides decision tree, support vector machine, random forest, and gradient boosting decision tree to predict the H_2 storage capacity of 7444 CoRE MOFs [94]. Deliverable H_2 capacities of MOFs between 100 bar, 77 K and 5 bar, 160 K were computed by GCMC simulations and the good prediction ability of CGCNN model was shown with 1000 hypothetical MOFs and 5 experimental MOFs. Given the vast number of hypothetical MOFs which is likely to increase, the fast prediction of H_2 storage performances with CGCNN as explained in that work is projected to be highly helpful for the initial screening of novel MOFs.

A different route to input the full structural information of a MOF to the ML model is to describe the structure as an array including information for their nodes, linkers, and topologies. MOFid and MOFkey [95] are string form identifiers derived from Simplified Molecular Input Line Entry System (SMILES) and International Chemical Identifier (InChiKey), respectively, which provide a means to represent molecular graphs in barcode-like forms and they were used to extract information from MOF building blocks as well as topology [96]. Feature embedding was coupled with molecular graph convolution to include both chemical and geometric information of MOFs in ML models. Comparison of ML predictions with the results of GCMC simulations for H_2 uptakes of 9156 hypothetical MOFs has shown that incorporating the chemical information of MOFs to the ML model is especially important to predict the H_2 uptakes at low pressure (2 bar, 77 K).

The descriptors used in ML integrated analysis of MOFs evolved with time to include the interaction energies between H_2 and MOFs. A new descriptor, potential energy landscape of MOF-H_2 interaction, was designed to reduce the interplay of several structural and chemical properties down to a single factor and to rapidly predict volumetric H_2 storage capacity of 54,776 hypothetical and synthesized MOFs [97]. Potential energy landscape was obtained from RASPA simulation software [98] as a three dimensional map of MOF−H_2 interaction energies and converted into one dimensional energy histograms. The use of energy histogram in the Least Absolute Shrinkage and Selection Operator regression models at adsorption and desorption conditions revealed that strong binding sites generally governed the uptake at desorption pressure, whereas mild binding sites designate how much pore space could be used at high pressures for adsorption to improve the net storage of hydrogen. With the ML model, the top 1000 MOFs with the highest deliverable H_2 capacities were identified and one of these materials with a promising deliverable H_2 capacity (MFU-4*l*) was finally synthesized. MFU-4*l* was reported to have high deliverable H_2 capacities, 36 g/L between 100 bar and 2 bar at 77 K, and 47 g/L between 100 bar, 77 K and 5 bar, 160 K. Thus, the collaboration between computational screening, ML, and experimental investigation established a complete framework for the discovery of a new MOF material.

Most of the works on H_2 storage performances of MOFs consider 77 K since H_2 interacts more strongly with the framework at low temperatures. However, it would be more practical to achieve high deliverable H_2 capacities at room temperature. The deliverable H_2 capacity of MOFs is a result of mainly three different H_2 adsorption mechanisms: H_2 adsorbed by contacting the metal sites, H_2 forming a monolayer by contacting the pore walls, and mid-pore H_2 filling the pores. Therefore, the strength of interaction of H_2 to the framework is an important factor affecting the deliverable capacities of MOFs. Since catecholate (a benzenediol) sites were previously shown to play a significant role on increasing the interaction of H_2 with the framework at room temperature [99,100]. GCMC simulations and a neural network model were combined to investigate the deliverable volumetric H_2 capacity of 105 different hypothetical MOFs with alchemical catecholate sites [101]. The maximum deliverable H_2 capacity of materials was predicted with high accuracy using the descriptors void fraction, framework density, pore size, surface area, number density of alchemical catecholate sites, energy parameter for H_2-alchemical site interaction, temperature, and pressure. It was shown that artificial models like the neural network model greatly facilitate the investigation of how operating conditions and adsorbent design could be optimized together to increase the deliverable volumetric H_2 capacity of each adsorbent. The deliverable H_2 capacity of 2736 hypothetically constructed Zr-MOFs with metal catecholate groups were also investigated between 100 bar and 5 bar at room temperature [102]. In this case, a random forest model was used to assess the relative significance of various descriptors including pore limiting diameter, largest cavity diameter, void fraction, surface area, and theoretical maximum H_2 capacity (estimated with assuming that $4H_2$ molecules would adsorb per metal site in the MOF). Surface area was highlighted as the most important descriptor for predicting gravimetric and volumetric H_2 capacity with random forest model. These findings highlighted the potential for identifying novel descriptors to understand H_2 adsorption mechanisms in MOFs.

Post-synthetic modification is one of the means to enhance H_2 storage performances of MOFs; however, it is not straightforward to decide how each strategy would contribute to the performance of a MOF. For example, functionalization of MOFs might enhance the MOF−H_2 interaction, but it would be with a sacrifice from available pore volume; therefore, overall effect of functionalization on deliverable H_2 capacity of the MOF is difficult to predict. Combining computational screening with ML provides an extremely helpful tool to assess how the functionalization of a MOF would affect its H_2 storage performance. In an example case, benzene rings of IRMOF-8, IRMOF-14, and IRMOF-16 were functionalized to enhance volumetric and gravimetric H_2 uptakes of materials, and ML was used to predict the interaction energy of H_2 with the functional groups [103]. A set of 1000 data points was used to show that ML models kernel ridge, random forest, and support vector machine were able to predict binding energies using coulomb matrix, bag of bonds, and smooth overlap of atomic potentials as the descriptors.

The very comprehensive dataset of 820,039 experimentally synthesized and hypothetical MOFs was analyzed using extremely randomized trees model and four output properties, gravimetric and volumetric deliverable H_2 capacities of MOFs under pressure swing and temperature−pressure swing conditions, were predicted as shown in Fig. 5(a-b) [104]. Simple descriptors such as single-crystal density, pore volume, gravimetric and volumetric surface area, void fraction, largest cavity diameter, and pore limiting diameter were used for the model. Results showed that to predict gravimetric deliverable H_2 capacity of a MOF under pressure swing conditions, gravimetric surface area and void fraction are needed in addition to the largest cavity diameter, pore limiting diameter, and pore volume of the MOF, while volumetric surface area and density are essential instead of gravimetric surface area and void fraction to make predictions for the temperature−pressure swing conditions. The models developed in that work were made available through a web-based tool which will facilitate wide usage for non-experts on data science to acquire insights from ML-based research and to predict the H_2 storage performances of new MOFs [105].

Adsorption isotherm functions such as Langmuir and dual-site Langmuir are highly useful to model adsorption behavior of a gas. These functions must be fitted for each adsorbent-gas system separately while a generalized model that is applicable to all adsorbent-gas systems would significantly facilitate the prediction of gas storage capacities of materials at different operating conditions. A meta-learning model that learns from the adsorption isotherm functions was developed to provide generalized adsorption predictions for novel materials based on a huge set of adsorption data; the results of GCMC simulations for adsorption of H_2 at 64 different pressure−temperature combinations in 531 different nanoporous materials including zeolites and MOFs [106]. The developed model was shown to predict adsorption loadings with higher accuracy than adsorption isotherm functions, which will pave the way for the rapid prediction of optimal temperature and pressure conditions for a high H_2 working capacity of a unique nanoporous material.

The shape of an adsorption isotherm also provides significant information about the temperature and pressure required for a material to attain saturation, which may then be utilized to determine optimal adsorption and desorption conditions for a high deliverable H_2 capacity. A novel approach based on the energetics of adsorption was developed by combining ML with GCMC for the quick determination of the full adsorption isotherm of H_2 in MOFs [108]. A mathematical model was developed as a function of MOF−H_2 and H_2−H_2 interaction energies and used to estimate H_2 uptake in a MOF as a function of energy distribution of adsorption sites. While a grid of MOF−H_2 interaction energy could be directly obtained from GCMC simulations, revealing the environment of H_2 inside pores and estimating the H_2−H_2 interaction energies at different pressures and temperatures were not straightforward. A Gaussian Process Regression (GPR) model was trained to estimate H_2−H_2 interaction energy through the coordination number of H_2 inside pores as a function of temperature, pressure, pore size, and porosity of MOFs. Combining MOF−H_2 interaction energy obtained from GCMC simulations with the predictions of GPR model for H_2−H_2 interaction energy, 13 MOFs that can exceed the DOE target for deliverable H_2 capacity of 50 g/L, among 12,914 CoRE MOFs [11], could be identified in a few hours.

Inverse material design is a valuable strategy for generating high-performing materials. Based on this idea, a natural language processing (NLP)-based model MOF-NET was proposed to design and construct MOFs with high CH_4 storage performances [109]. MOF-NET was recently employed in a method that combines ML with genetic algorithm to connect the information on MOF's building blocks with their deliverable volumetric H_2 capacity [107]. In this workflow, building blocks and topologies in the search space of randomly generated MOFs were transformed to vectors and fed into a neural network model which was trained using the results of GCMC simulations for volumetric H_2 capacities. As shown in Fig. 5(c), information on node and edge building blocks of MOFs with high volumetric H_2 capacities was fed into the genetic algorithm to identify materials with optimal H_2 storage properties. Fig. 5(d) shows that a significant number of structures among 132,209 generated MOFs has deliverable volumetric H_2 capacities superior to the maximum capacity obtained with experimental MOFs (37.2 g/L obtained with NPF-200 between 100 and 5 bar, at 77 K). Overall, this study offers an efficient method for designing and synthesizing novel MOFs having high volumetric H_2 capacities, which will be especially valuable for experimental researchers in this field.

Establishment of accurate ML models valid for several material classes such as COFs, zeolites, and porous polymer networks is considered as a more challenging task since available datasets for these materials are not as enormous as for MOFs. This motivated Kim et al. [110] to develop a “cross-material transfer learning” model based Porous Material Transformer which was also useful to reveal the relationships between different classes of materials. Atomistic information and properties related to crystalline structure of almost two million different porous materials were utilized to predict H_2 uptakes of materials while the model was first pre-trained to acquire how to represent input parameters in the most effective way. When the Porous Material Transformer was pre-trained with MOFs, H_2 uptakes of COFs and porous polymer networks at 100 bar, 77 K could be predicted with high accuracy thanks to the underlying relationships between the structural properties of MOFs and other material classes. This work is a significant step showing the importance of the establishment of ML models to predict H_2 storage performances of MOFs that are transferable to different types of porous materials.

3.2. H_2 separation

ML has just been integrated to HTCS for the investigation of H_2 separation performances of MOFs and studies in this field have just started to appear. For example, genetic algorithm was utilized to identify promising MOF candidates among 55,163 hypothetical MOFs for adsorption-based CO_2/H_2 separation [111]. Each hypothetical MOF was represented as a chromosome, where genes carried information on the interpenetration capacity, interpenetration level, identities of the node and linker types, and functional groups. This information was paired with target properties such as selectivity, working capacity, and adsorbent performance score which were calculated using the gas uptakes obtained from GCMC simulations for CO_2/H_2 mixture. Range of structural properties obtained using the genetic algorithm for high selectivity, working capacity, and adsorbent performance scores were utilized to identify a promising MOF, NOTT-101/OEt, which was then synthesized and shown to have a good CO_2/H_2 separation performance by experiments.

It is difficult to evaluate the membrane-based separation performances of very large number of materials since neither experimental fabrication of each membrane nor computation of the transport parameters of gases in each structure is practical. ML has a huge potential to quickly scrutinize the top membrane materials among enormous number of candidates for H_2 purification applications and the field is just emerging. Performances of CoRE MOF membranes for H_2/CH_4, H_2/N_2, H_2/H_2S, H_2/O_2, H_2/CO_2, and H_2/He separations were recently studied using HTCS and ML. The structural descriptors such as pore limiting diameter, largest cavity diameter, volumetric surface area, porosity, density, and the

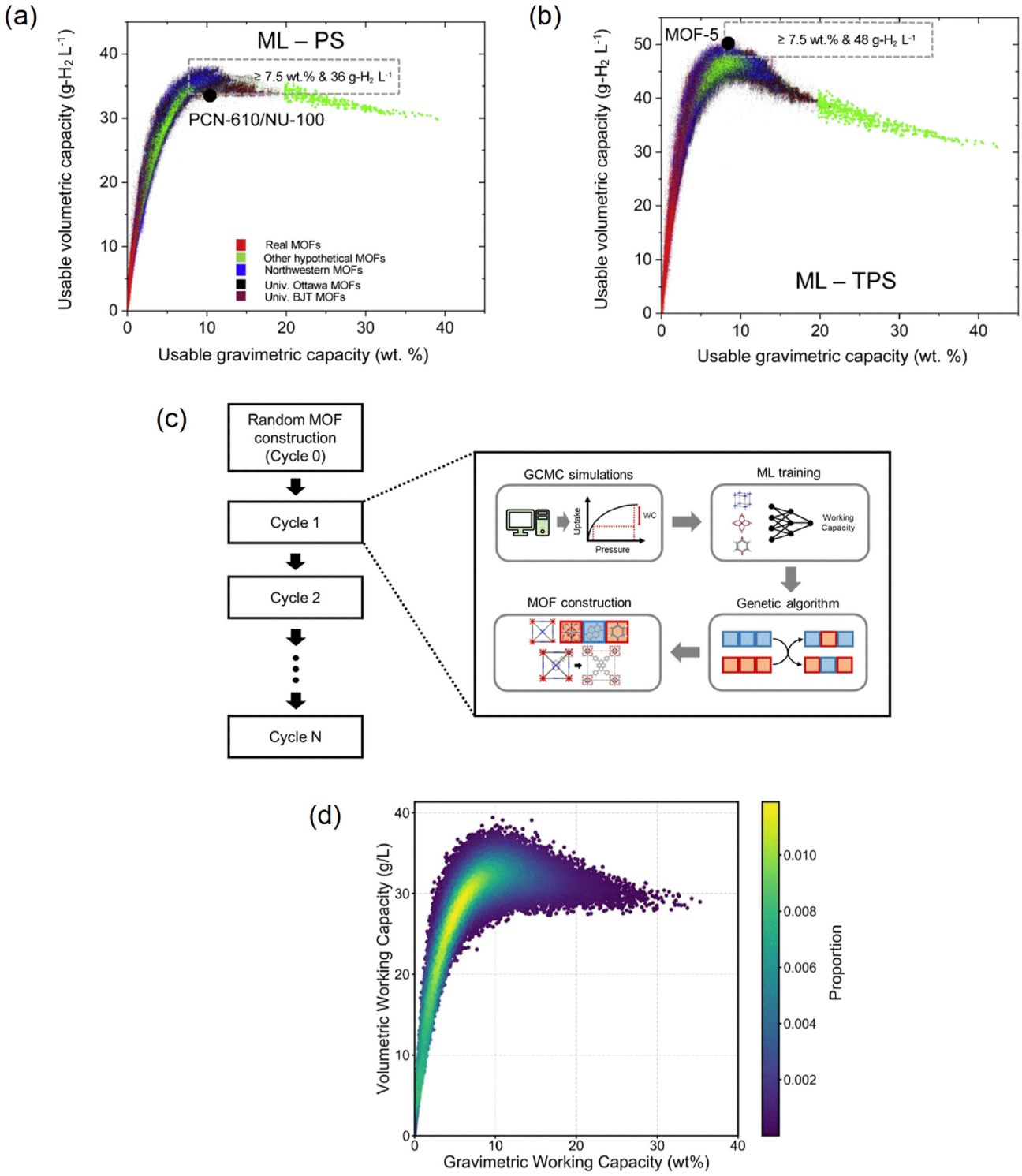


Fig. 5. Predictions for deliverable volumetric and gravimetric H_2 capacity of 820,039 hypothetical and experimentally synthesized MOFs at (a) pressure swing (PS) and (b) temperature–pressure swing (TPS) conditions. Colors represent various MOF databases studied in that work. MOFs in gray dashed-line boxes overcome the performances of previously identified benchmark MOFs, PCN-610/NU-100 at PS condition, and MOF-5 at TPS condition. Figures reprinted from the study by Ahmed and Siegel [104] with permission from Elsevier. (c) MOF construction based on genetic algorithm. Figure reprinted with permission from the study by Park et al. [107] Copyright 2022 American Chemical Society. (d) Deliverable volumetric and gravimetric H_2 capacities of 65,322 generated MOFs between 100 and 5 bar, at 77 K. Figure reprinted with permission from the study by Park et al. [107] Copyright 2022 American Chemical Society. MOF, metal-organic framework.

distribution of pore sizes were used to develop 8 different ML models that can predict H_2 permeability and trade-off between permeability and selectivity of membranes. Via comparing the ML predictions with the values computed with GCMC and EMD simulations, Gaussian progress regression and random forest models were selected as the top performing models to assess the membrane-based H_2 separation performances of CoRE MOFs. Pore limiting diameter (volumetric surface area) was found as an

important descriptor for estimating H_2 permeability (trade-off between permeability and selectivity) of membranes [112]. D_2/H_2 membrane selectivities of 12,723 CoRE MOFs computed at 77 K at infinite dilution condition with HTCS were used to establish support-vector machine models which were then used to identify the structural properties of MOFs for membrane-based separation of H_2 from D_2. The results showed that MOFs with a porosity between 0.4 and 0.5, PLD (pore limiting diameter) of ~2.5 Å, and LCD (largest cavity diameter) in the range of 3–5 Å lead to higher membrane-based D_2/H_2 separation performances [113].

Given that there are thousands of MOFs and hundreds of polymers, theoretically an infinite number of MOF/polymer MMMs can be generated. Accurate estimates of the gas separation performances of all these potential MMMs using ML models will greatly speed up the design and fabrication of new MMMs for various types of gas separations. Recently, H_2 permeabilities as well as H_2/N_2 and H_2/CH_4 selectivities of 5249 different types of MOF membranes and a total of 32,494 MOF/polymer MMMs were investigated using ML-predicted adsorption and diffusion data of gases in MOFs [114]. Among 20 different physical, chemical, and energy-based descriptors, porosity was shown to be more dominant to affect the adsorption (N_i) and diffusion (D_i) of gases than other descriptors (such as percentage of the elements in a MOF, density, pore volume, surface area etc. as shown in Fig. 6) as shown the width range of the corresponding boxes. The results of this work demonstrate that the approach of predicting gas adsorption and diffusion properties via ML would highly facilitate the prediction of membrane-based H_2/N_2 and H_2/CH_4 separation performances of MOF membranes and MOF/polymer MMMs and direct experimental efforts to the most promising MMM candidates.

4. Outlook

ML has already facilitated the extraction of hidden patterns from a massively high dimensional data space which might not be trivial to comprehend through conventional analysis methods in field of MOFs. ML-based research can open new horizons for H_2 storage and separation systems by studying system integration and optimization, cost, scalability, and safety. We believe that focusing on the following topics will be essential, while we take full advantage of ML-assisted material discovery for the future of H_2-based energy solutions.

4.1. Data management

Scientific data must systematically accumulate for science to advance, which highly necessitates precise data management. The life-cycle of planning, collecting, analyzing, managing, publishing, and reuse of data mandates a digital curation strategy to make data available for reuse even after years [115]. As we have reviewed, ML studies depend on high quality, diverse, and curated data while the outcomes of HTCS studies are mostly used. Therefore, process of ML-based research for any application completely depends on data management and data accessibility, and tools which aid the management and sharing of data are critical for the success of this field. The FAIR (findability, accessibility, interoperability, and reusability) principles were published in 2016 as a guideline for data management [116], and adherence to these criteria is expected to improve the rigorous use of data in ML-assisted materials research. Most of the experimental and computational data available on H_2 storage in MOFs are about structural properties (such as surface area and pore volume) of materials and their gas uptakes at different operating conditions, mostly in the form of tables or figures, but these formats are not easily readable for the tools of ML, yet. NLP has been recently very useful in extracting surface area and pore volume of MOFs from the experimental literature [117], in processing elemental composition of MOFs to ML models in the form of word embedding [118], and in obtaining solvent-removal stability and thermal degradation temperatures of MOFs [119,120]. For instance, solvent-removal-based stability and thermal degradation temperatures were extracted from 3809 manuscripts describing 7004 MOFs via using NLP and image analysis. GPR and artificial neural network models which use structural and geometrical properties such as the pore geometry, type of linkers, and functional groups of MOFs as the descriptors and stability data as the target were then developed to be further used in engineering MOFs with high stability [119]. Pre-trained language models were also used to create knowledge graphs on MOFs combining information for the same MOF from multiple distinct sources [121] and data digitization tools were utilized to extract a large collection of mixture adsorption data in MOFs from tables and figures [122]. These

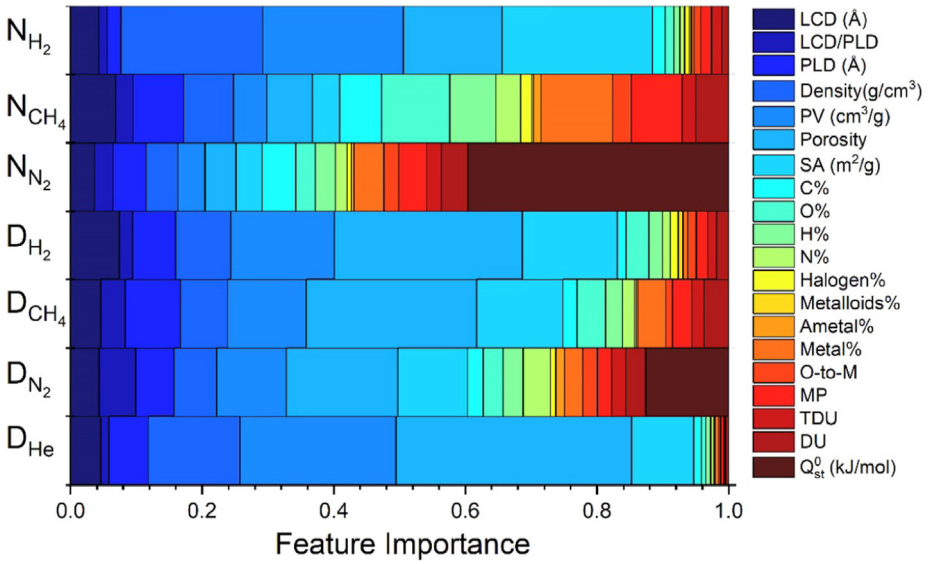


Fig. 6. Variation in importance of features for predicting the adsorption (N_i) and diffusion (D_i) of gases in MOFs with ML. Figure reprinted with permission from the study by Daglar and Keskin [114] (licensed under CC BY 4.0). ML, machine learning; MOF, metal organic framework.

approaches facilitate the access to data but generally demand high manual effort as well as expertise in computer science and data science. In this respect, recently, adsorption information file format (AIF) was proposed for the standardized documentation and easy accessibility of experimentally and computationally obtained gas uptakes [123]. We expect similar approaches to be widely adopted which will be extremely helpful for the accessibility, replication, and utilization of scientific data by other research groups. At this point, it is important to discuss the enormous MOFX-DB in which simulated H_2 uptakes in over 160,000 MOFs and 286 zeolites are documented in addition to their structure files. These approaches would facilitate the reproducibility of ML models by different research groups [124]. If data for system configuration, equipment design, control parameters, and sensor activities can be collected, there is a huge potential for ML to be applied for the scalability, safety, and maintenance of H_2 storage systems.

4.2. Selection of MOF database

Before performing molecular simulations, multiple steps are required such as removal of solvents and completion of missing hydrogen atoms to obtain MOFs and COFs as computation-ready structures. There are cases that a MOF can be curated differently during these steps and included in different MOF databases with the same name but with different structures. Therefore, the database used in HTCS studies affect the identification of the most promising MOF candidates for H_2 storage. A computational analysis on 1109 MOFs have shown that the presence of halogen groups or guest molecules like H_2 and D_2 inside pores significantly affect the H_2 uptakes of MOFs especially at low pressures (infinite dilution and 1 bar) [125]. The investigation of MOFs with identical names but structural differences in different databases for the purification of H_2 from CH_4 has shown that the ranking of MOFs based on performance evaluation metrics such as selectivity and regenerability are also affected by the selection of the MOF database [126]. For ML-based analysis, the identity of a MOF is an array of its chemical and structural properties. Therefore, we believe the results of an ML study focusing on a specific computation-ready database should be interpreted with caution, given the structural discrepancies between multiple MOF databases.

4.3. Design and synthesis of new MOFs with inverse engineering

We reviewed examples of high-performing MOFs which were first identified by computational methods and then experimentally investigated for H_2 storage such as SIFSIX-18-Cd and MFU-4*l*. An enormous number of promising materials are waiting in line for a similar procedure. Structural and chemical features that are revealed in ML-assisted discovery of MOFs and COFs can be helpful to further narrow down this material space. Structural tunability is a key aspect that makes MOFs and COFs attractive for H_2 storage and evolution of new tools that will easily redesign MOF and COF structures will be very useful. A recent example is the open-source Python package, MOFUN, which can be used to easily modify a MOF with a molecular find and replace algorithm [127]. Another important factor to also consider is that several works using ML rely on the chemical and structural properties of hypothetical materials; however, it is not exactly clear if a synthesis procedure will be available for these materials. With the innovations in robotics, artificial intelligence, and computer science, now discovery of novel materials can benefit more from smart automation as was previously discussed [128,129]. This will especially support the inverse design, targeting a synthesis procedure based on a crystal structure, for the synthesis of materials with pre-defined properties. With the recently proposed tool MOFormer [130], it is now also possible to make MOF property prediction using the string representation of hypothetical MOFs instead of their 3D structures.

If ML predictions on optimal synthesis conditions are combined with the workflow of computational prediction of high performing materials, the experimental realization of the most promising materials will be significantly accelerated. DigiMOF [131], an online database obtained as a result of text-mining 43,281 unique MOF publications, provides an effective tool to examine alternative pathways for MOF production. Similarly, SynMOF database composed of 983 MOFs provides a large amount of data to be used in ML studies to predict synthesis conditions depending on a crystal structure [132]. Recently, a ChatGPT-based Chemistry Assistant workflow, obtained via combining prompt engineering with an NLP tool, ChatGPT, has been shown to be able to extract experimental synthesis conditions such as the such as the synthesis method (solvothermal, microwave-assisted, etc.), metal/linker/solvent/modulator types and amounts, reaction temperature, and reaction time, from the scientific literature with high precision. Random forest models that can predict the crystal morphological characteristics of MOFs, polycrystalline or single crystal, based on the synthesis conditions were then developed [133]. These advancements signal that with the collaboration of text mining, NLP, and ML, it will soon be a much trivial task to design a synthesis protocol that yields to single crystal MOFs to be used in H_2 storage applications. Except from the synthesis of the complete structure, ML can also be used to define the cost-effective synthesis conditions with minimal waste for the linkers of MOFs and COFs via utilizing the information on known reactions and molecules provided in accessible databases [134,135]. The recent example of COF synthesis utilizing ML for solvent screening is promising [136]. It is also important to record failed synthesis experiments as well as successful ones for the automated discovery of these materials. We expect these efforts will significantly change the routine for experimental discovery of materials for H_2 storage and separation applications.

4.4. Kinetics of adsorption/desorption

Fast kinetics of H_2 through adsorbents is required for the efficient operation of adsorption/desorption cycles and plays a significant role on achieving a high deliverable capacity in a given time. However, there is limited number of works investigating the kinetic properties of gases inside adsorbents. ML tools can be combined with the results of EMD and NEMD simulations as well as breakthrough experiments to provide an understanding of mass transfer limitations.

4.5. ML for computational investigation

Molecular modeling and ML are two fields that can collaborate and advance one another. One of the aspects that ML should be utilized more frequently in the advancement of computational investigation is the derivation of force fields. Force fields are essential to describe the interaction of H_2 with MOFs and COFs in molecular simulations and parameters are generally derived depending on ab-initio calculations or experimental data such as vapor-liquid equilibrium curves. However, under specific conditions generic force fields might not be able to adequately describe adsorption of H_2 in a MOF. For example, describing the interaction of H_2 with adsorbents at low temperatures like 77 K is considered to be beyond the scope of classical physics and corrections like Feynman-Hibbs correction are required in addition to the interactions described by the force field [137]. At this point, ML can be utilized to derive force field parameters that can better describe the interaction of H_2 with MOFs and COFs under various circumstances

including low temperature and high pressures as well as in flexible structures or in structures with defects. ML must be predictive but also interpretable and reproducible while ML models should not suggest H_2 capacities that cannot be reached at thermodynamically available conditions.

We believe that integration of ML with molecular simulations and experiments will provide a better understanding of material properties and operating conditions that would eventually help to reach the ultimate potential of MOFs and COFs in H_2 storage and separation applications.

Credit author statement

Seda Keskin: Supervision, Funding acquisition, Conceptualization, Writing-Reviewing and Editing. Cigdem Altintas: Conceptualization, Writing-Original Draft, Reviewing and Editing.

Declaration of competing interest

The authors declare that they have no known competing financial interests or personal relationships that could have appeared to influence the work reported in this paper.

Data availability

This is a review paper.

Acknowledgments

S.K. acknowledges ERC-2017-Starting Grant. This study has received funding from the European Research Council (ERC) under the European Union's Horizon 2020 research and innovation programme (ERC-2017-Starting Grant, grant agreement no. 756489-COSMOS). The authors declare no competing financial interest.

References

[1] I. Staffell, D. Scamman, A. Velazquez Abad, et al., Energy Environ. Sci. 12 (2) (2019) 463.
[2] H.-J. Lin, H.-W. Li, H. Shao, et al., Mater. Today Energy 17 (2020) 100463.
[3] Q.-W. Deng, G.-Q. Ren, Y.-J. Li, et al., Mater. Today Energy 18 (2020) 100506.
[4] Hydrogen Storage Engineering Center of Excellence | Department of Energy. Hydrogen Storage Engineering Center of Excellence | Department of Energy, Vol. vol. 2023.
[5] DOE Technical Targets for Onboard Hydrogen Storage for Light-Duty Vehicles vol. 2023, US Department of Energy Office of Energy Efficiency and Renewable Energy, 2017.
[6] P. Jena, J. Phys. Chem. Lett. 2 (3) (2011) 206.
[7] K.O. Kirlikovali, S.L. Hanna, F.A. Son, et al., ACS Nanosci. Au 3 (1) (2023) 37.
[8] X. Zhang, Z. Chen, X. Liu, et al., Chem. Soc. Rev. 49 (20) (2020) 7406.
[9] Z. Ji, H. Wang, S. Canossa, et al., Adv. Funct. Mater. 30 (41) (2020) 2000238.
[10] M.D. Allendorf, R. Dong, X. Feng, et al., Chem. Rev. 120 (16) (2020) 8581.
[11] Y.G. Chung, E. Haldoupis, B.J. Bucior, et al., J. Chem. Eng. Data 64 (12) (2019) 5985.
[12] P.Z. Moghadam, A. Li, X.-W. Liu, et al., Chem. Sci. 11 (32) (2020) 8373.
[13] P.Z. Moghadam, A. Li, S.B. Wiggin, et al., Chem. Mater. 29 (7) (2017) 2618.
[14] C.E. Wilmer, M. Leaf, C.Y. Lee, et al., Nat. Chem. 4 (2) (2012) 83.
[15] Y.J. Colón, D.A. Gomez-Gualdron, R.Q. Snurr, Cryst. Growth Des. 17 (11) (2017) 5801.
[16] P.G. Boyd, T.K. Woo, CrystEngComm 18 (21) (2016) 3777.
[17] P. García-Holley, B. Schweitzer, T. Islamoglu, et al., ACS Energy Lett. 3 (3) (2018) 748.
[18] M. Hirscher, L. Zhang, H. Oh, Appl. Phys. 129 (2) (2023) 112.
[19] D.A. Gomez-Gualdron, T.C. Wang, P. Garcia-Holley, et al., ACS Appl. Mater. Interfaces 9 (39) (2017) 33419.
[20] M. Fischer, F. Hoffmann, M. Froba, ChemPhysChem 10 (15) (2009) 2647.
[21] B. Panella, M. Hirscher, H. Pütter, et al., Adv. Funct. Mater. 16 (4) (2006) 520.
[22] S.S. Kaye, A. Dailly, O.M. Yaghi, et al., JACS 129 (46) (2007) 14176.
[23] Hydrogen Storage Engineering Center of Excellence, Department of Energy, 2023 (p Hydrogen Storage Engineering Center of Excellence | Department of Energy).
[24] M.J. Thornton, L.J. Simpson, System Design, Analysis, and Modeling Activities Supporting the DOE Hydrogen Storage Engineering Center of Excellence (HSECoE): Final Project Report, National Renewable Energy Lab.(NREL), Golden, CO (United States), 2019.
[25] K. Sumida, M.R. Hill, S. Horike, et al., JACS 131 (42) (2009) 15120.
[26] A.G. Wong-Foy, A.J. Matzger, O.M. Yaghi, JACS 128 (11) (2006) 3494.
[27] X. Feng, X. Ding, D. Jiang, Chem. Soc. Rev. 41 (18) (2012) 6010.
[28] O.M. Yaghi, M.J. Kalmutzki, C.S. Diercks, Introduction to Reticular Chemistry: Metal-Organic Frameworks and Covalent Organic Frameworks, John Wiley & Sons, 2019.
[29] D. Ongari, A.V. Yakutovich, L. Talirz, et al., ACS Cent. Sci. 5 (10) (2019) 1663.
[30] M. Tong, Y. Lan, Q. Yang, et al., Chem. Eng. Sci. 168 (2017) 456.
[31] K.S. Deeg, D. Damasceno Borges, D. Ongari, et al., ACS Appl. Mater. Interfaces 12 (19) (2020) 21559.
[32] J.S. De Vos, S. Borgmans, P. Van Der Voort, et al., J. Mater. Chem. A 11 (14) (2023) 7468.
[33] Y. Lan, X. Han, M. Tong, et al., Nat. Commun. 9 (1) (2018).
[34] D. Cao, J. Lan, W. Wang, et al., Angew. Chem. Int. Ed. 48 (26) (2009) 4730.
[35] S.S. Han, H. Furukawa, O.M. Yaghi, et al., JACS 130 (35) (2008) 11580.
[36] H. Furukawa, O.M. Yaghi, JACS 131 (25) (2009) 8875.
[37] M.D. Allendorf, Z. Hulvey, T. Gennett, et al., Energy Environ. Sci. 11 (10) (2018) 2784.
[38] N. Sinha, S. Pakhira, Mol. Syst. Des. Eng. 7 (6) (2022) 577.
[39] P. Peng, A. Anastasopoulou, K. Brooks, et al., Nat. Energy 7 (5) (2022) 448.
[40] Z.J. Chen, K.O. Kirlikovali, K.B. Idrees, et al., Chem 8 (3) (2022) 693.
[41] S. Keskin, J. Liu, R.B. Rankin, et al., Ind. Eng. Chem. Res. 48 (5) (2009) 2355.
[42] T. Düren, Y.-S. Bae, R.Q. Snurr, Chem. Soc. Rev. 38 (5) (2009) 1237.
[43] Y.G. Chung, J. Camp, M. Haranczyk, et al., Chem. Mater. 26 (21) (2014) 6185.
[44] C.R. Groom, I.J. Bruno, M.P. Lightfoot, et al., Acta Crystallogr. Sect. B Struct. Sci. 72 (2) (2016) 171.
[45] V. Buch, J. Chem. Phys. 100 (10) (1994) 7610.
[46] F. Darkrim, D. Levesque, J. Chem. Phys. 109 (12) (1998) 4981.
[47] A.K. Rappé, C.J. Casewit, K. Colwell, et al., JACS 114 (25) (1992) 10024.
[48] S.L. Mayo, B.D. Olafson, W.A. Goddard, J. Phys. Chem. 94 (26) (1990) 8897.
[49] M. Li, W. Cai, C. Wang, et al., Phys. Chem. Chem. Phys. 24 (31) (2022) 18764.
[50] G.O. Aksu, I. Erucar, Z.P. Haslak, et al., Chem. Eng. J. (2022) 427.
[51] H. Frost, T. Düren, R.Q. Snurr, J. Phys. Chem. B 110 (19) (2006) 9565.
[52] H. Frost, R.Q. Snurr, J. Phys. Chem. C 111 (50) (2007) 18794.
[53] Y.-S. Bae, R.Q. Snurr, Microporous Mesoporous Mater. 132 (1–2) (2010) 300.
[54] Y.-S. Bae, R.Q. Snurr, Microporous Mesoporous Mater. 135 (1–3) (2010) 178.
[55] J. Sculley, D. Yuan, H.-C. Zhou, Energy Environ. Sci. 4 (8) (2011) 2721.
[56] L. Zhang, M.D. Allendorf, R. Balderas-Xicohténcatl, et al., Prog. Energy. 4 (4) (2022) 042013.
[57] Y. Basdogan, S. Keskin, Cryst. Eng. Comm. 17 (2) (2015) 261.
[58] E. Ren, P. Guilbaud, F.-X. Coudert, Digital. Discovery. 1 (4) (2022) 355.
[59] J. Goldsmith, A.G. Wong-Foy, M.J. Cafarella, et al., Chem. Mater. 25 (16) (2013) 3373.
[60] R. Chahine, T. Bose, Int. J. Hydrogen Energy 19 (2) (1994) 161.
[61] P. Bénard, R. Chahine, Int. J. Hydrogen Energy 26 (8) (2001) 849.
[62] N.S. Bobbitt, J. Chen, R.Q. Snurr, J. Phys. Chem. C 120 (48) (2016) 27328.
[63] A. Ahmed, Y. Liu, J. Purewal, et al., Energy Environ. Sci. 10 (11) (2017) 2459.
[64] A. Ahmed, S. Seth, J. Purewal, et al., Nat. Commun. 10 (1) (2019) 1568.
[65] S. Majumdar, S.M. Moosavi, K.M. Jablonka, et al., ACS Appl. Mater. Interfaces 13 (51) (2021) 61004.
[66] Y.J. Colón, D. Fairen-Jimenez, C.E. Wilmer, et al., J. Phys. Chem. C 118 (10) (2014) 5383.
[67] D.A. Gomez, J. Toda, G. Sastre, Phys. Chem. Chem. Phys. 16 (35) (2014) 19001.
[68] D.A. Gómez-Gualdrón, Y.J. Colón, X. Zhang, et al., Energy Environ. Sci. 9 (10) (2016) 3279.
[69] C. Altintas, G. Avci, H. Daglar, et al., J. Mater. Chem. A 6 (14) (2018) 5836.
[70] C. Altintas, I. Erucar, S. Keskin, ACS Appl. Mater. Interfaces 10 (4) (2018) 3668.
[71] G. Avci, S. Velioglu, S. Keskin, ACS Appl. Mater. Interfaces 10 (39) (2018) 33693.
[72] A.N.V. Azar, S. Velioglu, S. Keskin, ACS Sustainable Chem. Eng. 7 (10) (2019) 9525.
[73] M.J. Chiau, Y.G. Wang, X.J. Wu, et al., Int. J. Hydrogen Energy 45 (51) (2020) 27320.
[74] Y. Chen, X. Bai, D. Liu, et al., ACS Appl. Mater. Interfaces 14 (21) (2022) 24980.
[75] C. Gu, Z. Yu, J. Liu, et al., ACS Appl. Mater. Interfaces 13 (9) (2021) 11039.
[76] J.H. Ren, W.J. Zeng, Y.L. Chen, et al., Sep. Purif. Technol. 295 (2022) 121286.
[77] H. Demir, S. Keskin, Mol. Syst. Des. Eng. 7 (12) (2022) 1707.
[78] O.F. Altundal, Z.P. Haslak, S. Keskin, Ind. Eng. Chem. Res. 60 (35) (2021) 12999.
[79] G. Avci, I. Erucar, S. Keskin, ACS Appl. Mater. Interfaces 12 (37) (2020) 41567.
[80] G.O. Aksu, H. Daglar, C. Altintas, et al., J. Phys. Chem. C 124 (41) (2020) 22577.
[81] S. Aydin, C. Altintas, S. Keskin, ACS Appl. Mater. Interfaces 14 (18) (2022) 21738.
[82] S. Aydin, C. Altintas, I. Erucar, et al., Ind. Eng. Chem. Res. 62 (6) (2023) 2924.
[83] S. Velioglu, S. Keskin, J. Mater. Chem. A 7 (5) (2019) 2301.
[84] N.S. Bobbitt, R.Q. Snurr, Mol. Simulat. 45 (14–15) (2019) 1069.
[85] L.T. Glasby, P.Z. Moghadam, Patterns 2 (7) (2021) 100305.
[86] H. Demir, H. Daglar, H.C. Gulbalkan, et al., Coord. Chem. Rev. 484 (2023) 215112.
[87] C. Altintas, O.F. Altundal, S. Keskin, et al., J. Chem. Inf. Model. 61 (5) (2021) 2131.
[88] S. Li, Y.G. Chung, C.M. Simon, et al., J. Phys. Chem. Lett. 8 (24) (2017) 6135.
[89] A.W. Thornton, C.M. Simon, J. Kim, et al., Chem. Mater. 29 (7) (2017) 2844.

[90] H. Furukawa, N. Ko, Y.B. Go, et al., Science 329 (5990) (2010) 424.
[91] I.A. Ibarra, S. Yang, X. Lin, et al., Chem. Commun. 47 (29) (2011) 8304.
[92] D. Yuan, D. Zhao, D. Sun, et al., Angew. Chem. Int. Ed. 49 (31) (2010) 5357.
[93] K.S. Park, Z. Ni, A.P. Côté, et al., Proc. Natl. Acad. Sci. USA 103 (27) (2006) 10186.
[94] X.Y. Lu, Z.Z. Xie, X.J. Wu, et al., Chem. Eng. Sci. 259 (2022) 15.
[95] B.J. Bucior, A.S. Rosen, M. Haranczyk, et al., Cryst. Growth Des. 19 (11) (2019) 6682.
[96] Z.H. Wang, Y.G. Zhou, T. Zhou, et al., Comput. Chem. Eng. 160 (2022) 11.
[97] B.J. Bucior, N.S. Bobbitt, T. Islamoglu, et al., Mol. Syst. Des. Eng. 4 (1) (2019) 162.
[98] D. Dubbeldam, S. Calero, D.E. Ellis, et al., Mol. Simulat. 42 (2) (2016) 81.
[99] E. Tsivion, J.R. Long, M. Head-Gordon, JACS 136 (51) (2014) 17827.
[100] E. Tsivion, S.P. Veccham, M. Head-Gordon, ChemPhysChem 18 (2) (2017) 184.
[101] G. Anderson, B. Schweitzer, R. Anderson, et al., J. Phys. Chem. C 123 (1) (2019) 120.
[102] H. Chen, R.Q. Snurr, J. Phys. Chem. C 125 (39) (2021) 21701.
[103] R.M. Giappa, E. Tylianakis, M. Di Gennaro, et al., Int. J. Hydrogen Energy 46 (54) (2021) 27612.
[104] A. Ahmed, D.J. Siegel, Patterns 2 (7) (2021) 100291.
[105] HyMarc Sorbent Machine Learning Model, National Renewable Energy Laboratory (NREL), 2023.
[106] Y. Sun, R.F. DeJaco, Z. Li, et al., Sci. Adv. 7 (30) (2021) eabg3983.
[107] J. Park, Y. Lim, S. Lee, et al., Chem. Mater. 35 (1) (2023) 9.
[108] A. Gopalan, B.J. Bucior, N.S. Bobbitt, et al., Mol. Phys. 117 (23–24) (2019) 3683.
[109] S. Lee, B. Kim, H. Cho, et al., ACS Appl. Mater. Interfaces 13 (20) (2021) 23647.
[110] Park, H., Kang, Y., Kim, J., (2023).
[111] Y.G. Chung, D.A. Gómez-Gualdrón, P. Li, et al., Sci. Adv. 2 (10) (2016) e1600909.
[112] X.N. Bai, Z.A. Shi, H. Xia, et al., Chem. Eng. J. 446 (2022) 11.
[113] M.S. Zhou, A. Vassallo, J.Z. Wu, J. Membr. Sci. 598 (2020) 9.
[114] H. Daglar, S. Keskin, ACS Appl. Mater. Interfaces 14 (28) (2022) 32134.
[115] C. Willoughby, J.G. Frey, Digital. Discovery. 1 (3) (2022) 183.
[116] M.D. Wilkinson, M. Dumontier, I.J. Aalbersberg, et al., Sci. Data 3 (1) (2016) 1.
[117] S. Park, B. Kim, S. Choi, et al., J. Chem. Inf. Model. 58 (2) (2018) 244.
[118] A.S. Krishnapriyan, J. Montoya, M. Haranczyk, et al., Sci. Rep. 11 (1) (2021) 8888.
[119] A. Nandy, C. Duan, H.J. Kulik, J. Am. Chem. Soc. 143 (42) (2021) 17535.
[120] A. Nandy, G. Terrones, N. Arunachalam, et al., Sci. Data 9 (1) (2022).
[121] Y. An, J. Greenberg, X. Hu, et al., Exploring Pre-trained language models to build knowledge graph for metal-organic frameworks (MOFs), in: Proceedings - 2022 IEEE International Conference on Big Data, Big Data 2022, 2022, p. 3651.
[122] X. Cai, F. Gharagheizi, L.W. Bingel, et al., Ind. Eng. Chem. Res. 60 (1) (2021) 639.
[123] J.D. Evans, V. Bon, I. Senkovska, et al., Langmuir 37 (14) (2021) 4222.
[124] N.S. Bobbitt, K. Shi, B.J. Bucior, et al., J. Chem. Eng. Data 68 (2) (2023) 483.
[125] H. Daglar, H.C. Gulbalkan, G. Avci, et al., Angew. Chem. Int. Ed. 60 (14) (2021) 7828.
[126] C. Altintas, G. Avci, H. Daglar, et al., J. Mater. Chem. A 7 (16) (2019) 9593.
[127] P. Boone, C.E. Wilmer, Digital. Discovery. 1 (5) (2022) 679.
[128] D.P. Tabor, L.M. Roch, S.K. Saikin, et al., Nat. Rev. Mater. 3 (5) (2018) 5.
[129] M.M. Flores-Leonar, L.M. Mejía-Mendoza, A. Aguilar-Granda, et al., Curr. Opin. Green Sustainable Chem. 25 (2020) 100370.
[130] Z. Cao, R. Magar, Y. Wang, et al., JACS 145 (5) (2023) 2958.
[131] L.T. Glasby, K. Gubsch, R. Bence, et al., Chem. Mater. 35 (11) (2023) 4510.
[132] Y. Luo, S. Bag, O. Zaremba, et al., Angew. Chem. Int. Ed. (19) (2022) 61.
[133] Z. Zheng, O. Zhang, C. Borgs, et al., J. Am. Chem. Soc. 145 (32) (2023) 18048.
[134] W.M. Barrett, S. Takkellapati, K. Tadele, et al., ACS Sustainable Chem. Eng. 7 (8) (2019) 7630.
[135] M.K. Yadav, New J. Chem. 41 (4) (2017) 1411.
[136] S. Kumar, G. Ignacz, G. Szekely, Green Chem. 23 (22) (2021) 8932.
[137] M. Wahiduzzaman, C.F. Walther, T. Heine, J. Chem. Phys. 141 (6) (2014) 064708.